

The Influence of Parallax Effects in Thick Silicon Sensors on Coherent Diffraction Imaging

M. Kuster ^a, R. Hartmann ^b, S. Hauf ^a, P. Holl ^b, T. Rüter ^{a,1}, L. Strüder ^b

^aData Department, European XFEL GmbH, Holzkoppel 4, 22869 Schenefeld, Germany

^bPNSensor GmbH, Otto-Hahn-Ring 6, 81739 München, Germany ¹On leave



Abstract

Structure determination is one of the most important application areas of 4th generation light sources. This method in particular can fully exploit the coherent and pulsed nature of the X-ray radiation delivered by X-ray free-electron lasers (XFEL) as the European XFEL. The focus of scientific interest in this area is understanding the physical, biological, and chemical properties of samples on the nanometer scale. The properties of the X-rays provided by the FEL enable Coherent X-ray Diffraction Imaging (CXDI), an experimental technique where a sample is irradiated with coherent X-rays and a far-field diffraction pattern is registered with an imaging detector.

By the nature of the underlying physics, the spatial resolution, at which the sample can be probed with the CXDI technique, is only limited by the wavelength of the X-ray radiation and the exposure time if a detector can record the diffraction pattern to very large solid angles.

The resolution that can be achieved under real experimental conditions, depends strongly on additional parameters. Amongst others, the Shannon pixel size, linked to the detector resolution, the coherent dose that can be deposited in the sample without changing its structure, the image contrast and the signal-to-noise ratio of the detected scattered radiation at high q , i.e. at high scattering angles 2θ , have a strong influence on the resolution. The signal-to-noise ratio at high q defines the “effective” maximum solid angle in a specific experiment setup up to which a detector can efficiently detect a signal and in consequence determines the achievable resolution. The image contrast defines how well bright image features can be distinguished from dark ones.

Point Spread Function

To describe the spatial response of an imaging detector to photons with an energy E impinging on the detector at an angle of incidence 2θ with the intensity $I_0(u, v)$, we use the Point Spread Function. With the PSF the intensity distribution of a point-like source as “seen” by the detector $I(x, y)$ is given by

$$I(x, y) = \iint_{-\infty}^{+\infty} I_0(u, v) \text{PSF}(x - u, y - v, E) du dv$$

The PSF fully describes the imaging response of the detector including e.g. charge collection, charge sharing, and the parallax effect depending on photon energy and the angle of incidence (AOI), i.e. the scattering angle 2θ .

Measured Point Spread Function

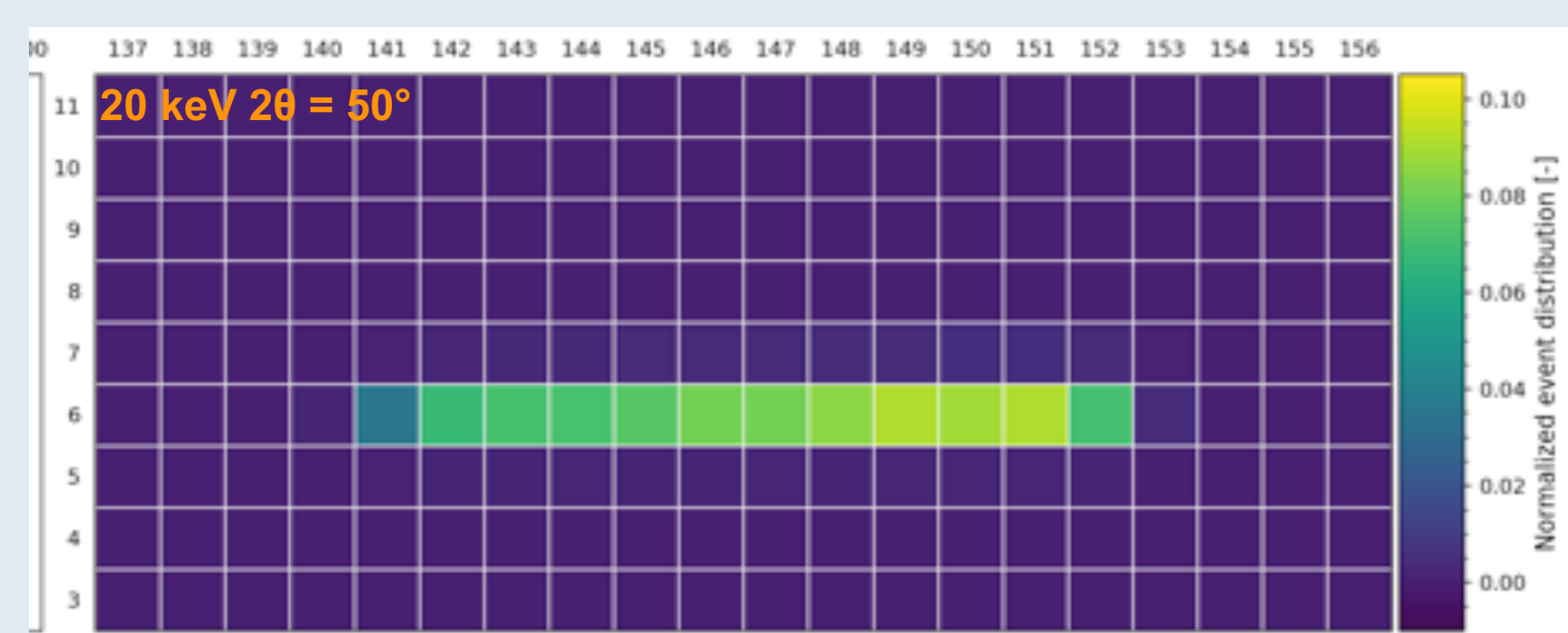


Figure 1: Exemplary PSF measured at 20 keV during a dedicated beamtime at the ESRF with a pnCCD detector with $75 \mu\text{m} \times 75 \mu\text{m}$ pixel size. The shape of the PSF is in qualitatively good agreement with the simulated PSF.

Image Contrast Depending on 2θ

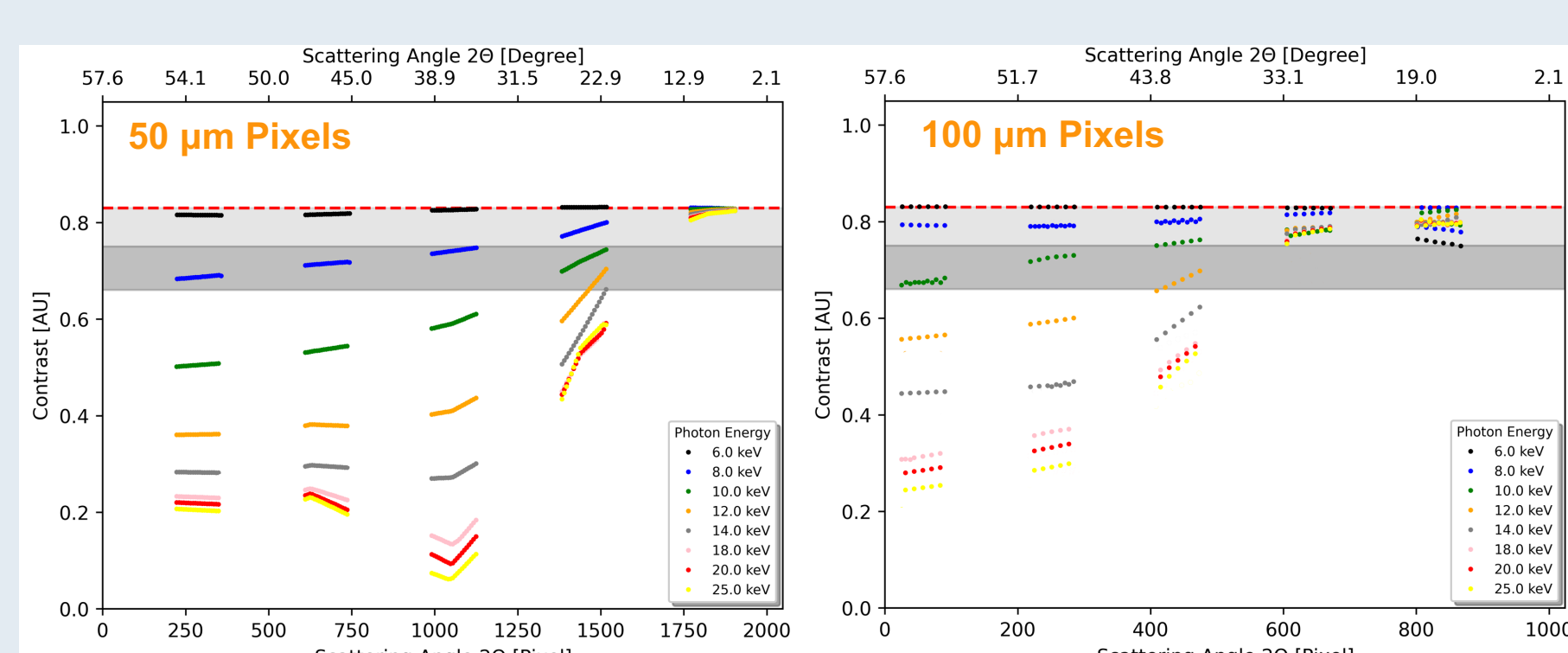


Figure 2: The image contrast derived from the line density patterns shown in Figure 5 as a function of photon energy and scattering angle 2θ is shown for two exemplary pixel sizes $50 \mu\text{m}$ (left) and $100 \mu\text{m}$ (right).

Parallax Effect

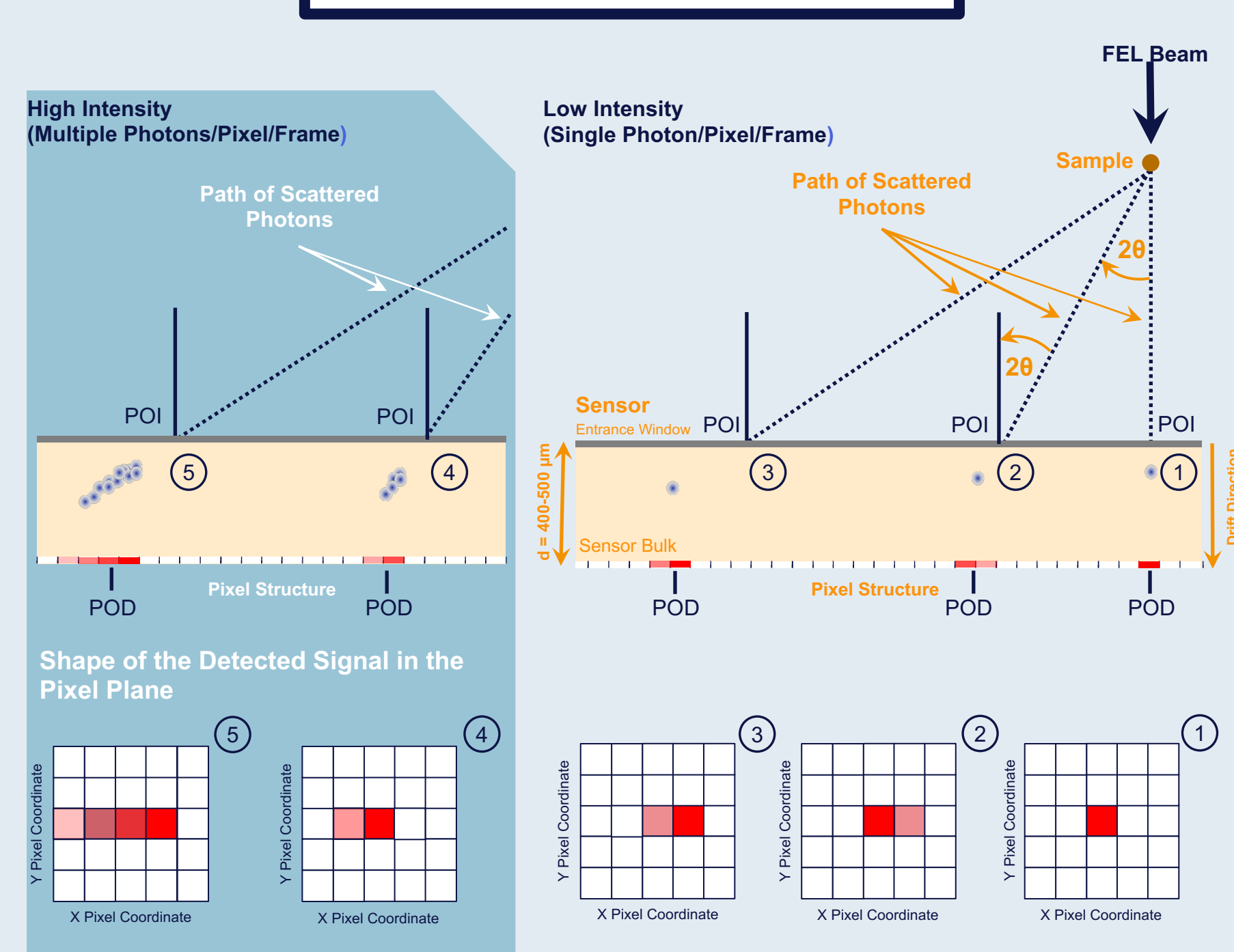
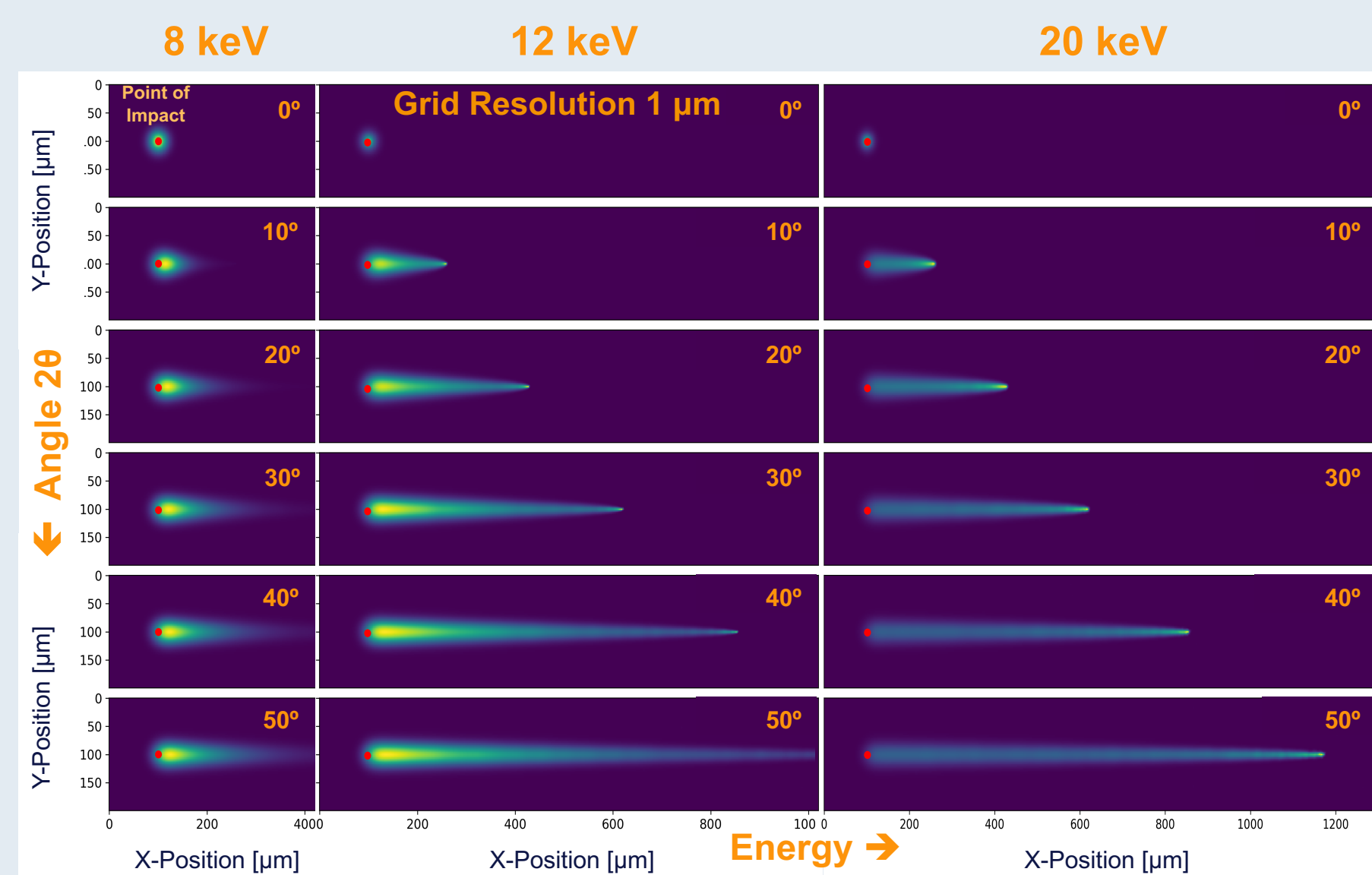


Figure 3: Expected signal morphology for single (right) and multiple photons (left) detected during one integration cycle. The detection geometry is illustrated depending on the scattering angle 2θ and the photon intensity. The remainder of this work is focused on the high intensity cases, i.e. an integrating detector system.

Point Spread Function Morphology



T. Rüter et al., IEEE NSS MIC (2017), pp. 1–3

Figure 4: Simulated shape of the Point Spread Function (PSF) depending on photon energy and scattering angle 2θ (AOI). The resolution of the PSF model is $1 \mu\text{m}$.

Imaging Resolution and Contrast

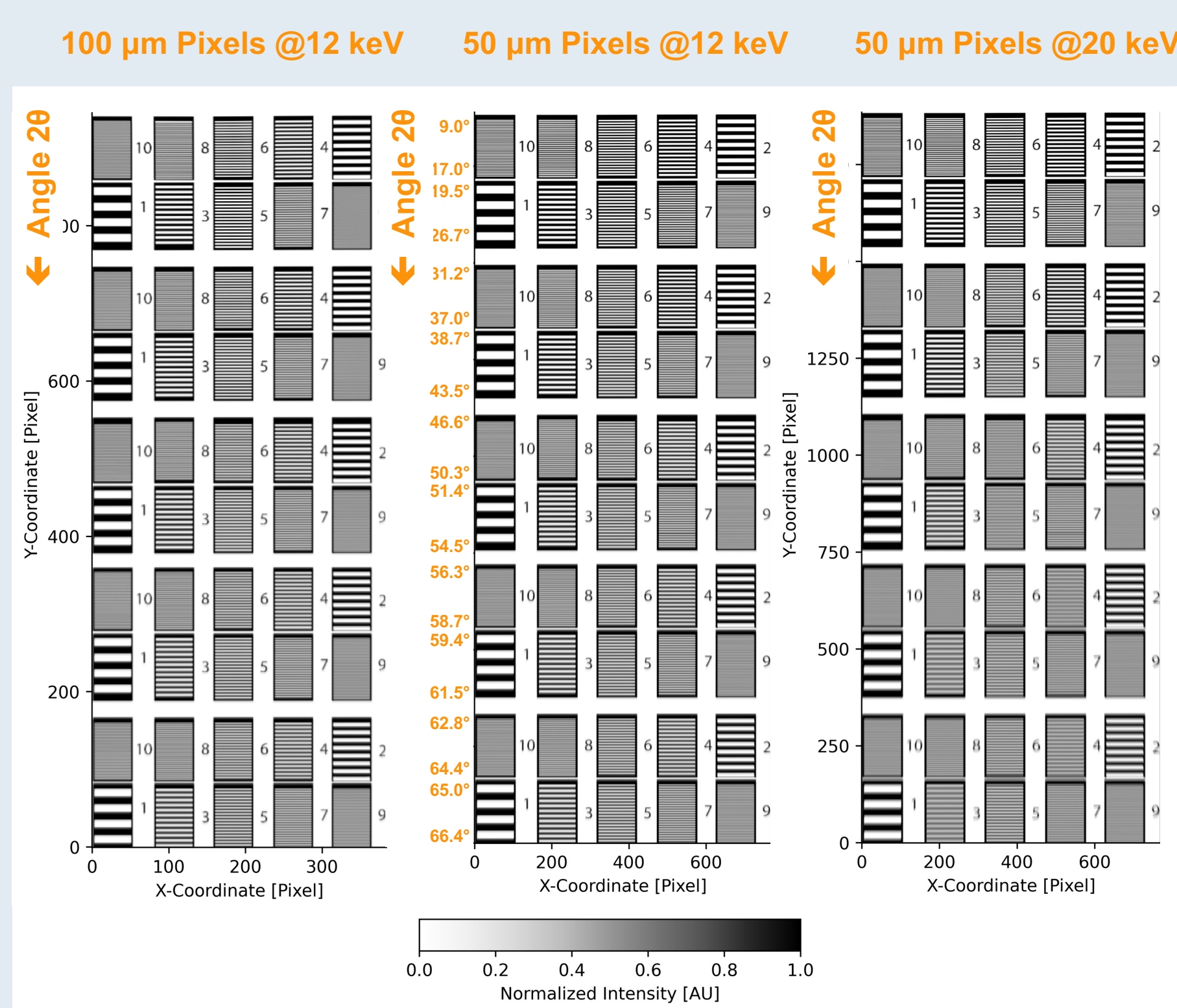


Figure 5: Simulated regular line density patterns convolved with our PSF model. We assume a planar detector geometry with a pixel size of $50 \mu\text{m}$ or $100 \mu\text{m}$. In this simulation, photons with an energy of 12 keV were used. The direct FEL beam hits the detector plane at normal incidence at position $y = 2048$ or 1024 , thereby defining the scattering angle $2\theta = 0.2\theta$ increases with decreasing y -values, i.e. towards the bottom.

Contribution of the Solid Angle

The solid angle extended by one pixel with the area A depends on the distance to the sample and is [2]

Simplified calculation

$$\Omega = \frac{A}{R^2}$$

A : Pixel area

Precise calculation

$$\Omega = \frac{A}{R} \cos^2(2\theta) \cos(\theta)$$

R : Distance sample to pixel

The signal amplitude decreases with increasing scattering angle 2θ proportional to the solid angle.

Detected Intensity per Pixel Area

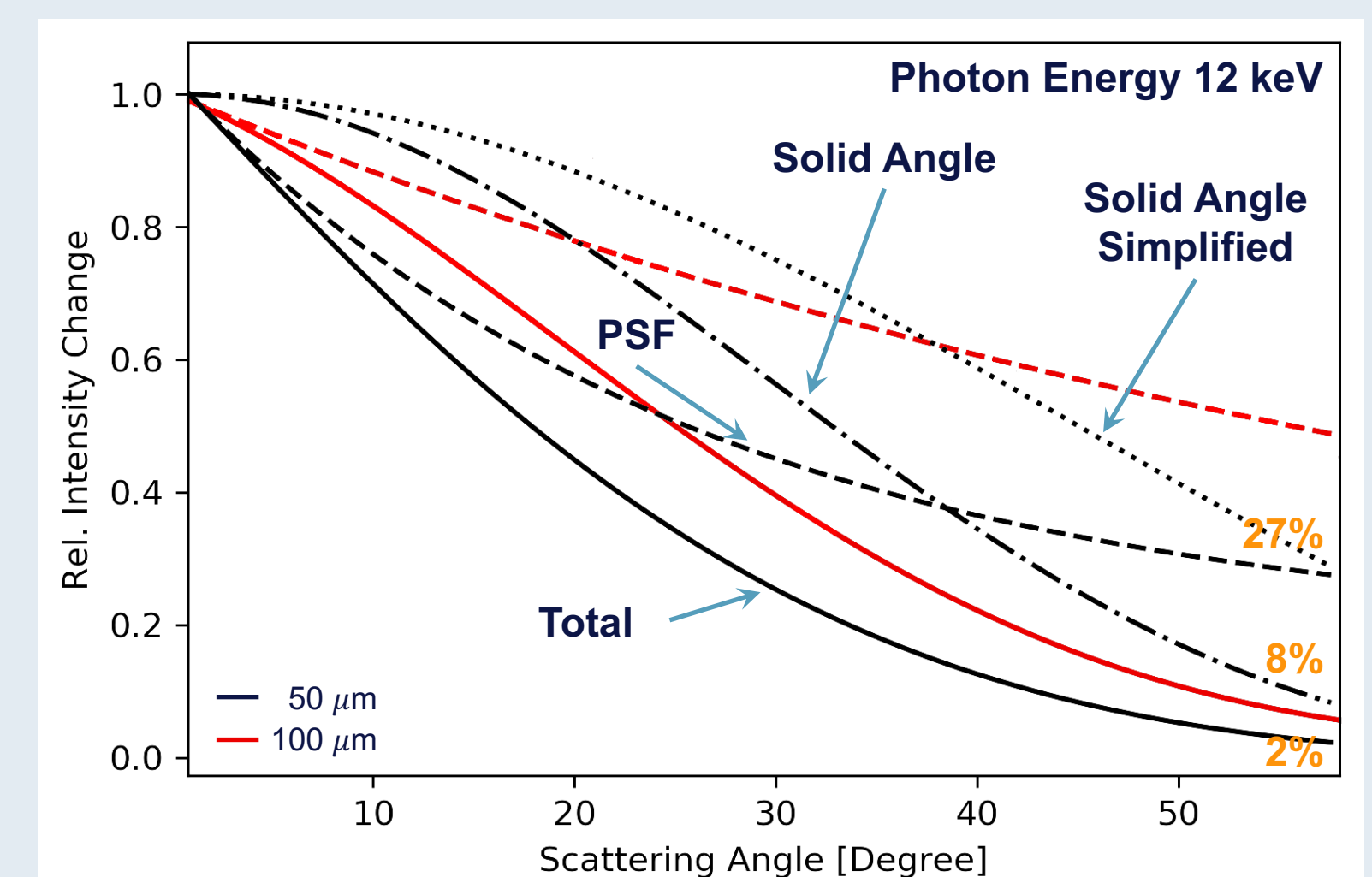


Figure 6: The relative change of the signal detected in a pixel depending on the scattering angle is shown for 12 keV photons, $50 \mu\text{m}$ (black), and $100 \mu\text{m}$ (red) pixel size for the high intensity case illustrated in Fig. 3.

The intensity drop with increasing scattering angle 2θ due to signal redistribution effect by the PSF can be well approximated by the analytical expression

$$I(2\theta) = I_c 10^{a \cdot 2\theta} \text{ with } I_c = I(2\theta = 0)$$

with $a = -1.7 \times 10^{-2}$ for $E = 12 \text{ keV}$ and $50 \mu\text{m}$ pixels. The parameter a depends on the photon energy and pixel size.

Relationship between the resolution and measured signal strength at q_{max}

The relation between the number of counts P detected during time Δt in the pixel corresponding to the resolution $d/2$ in the sample probed by a CDI experiment is given by [3, 4, 5, 6]

$$P \propto \frac{1}{8\pi^2 s^2} r_e^2 \lambda^2 d^4 \rho^2 I_0 \Delta t$$

with the complex electron density of matter $\rho = \sum_i n_{ai}(f_{1i} + if_{2i})$, the atomic concentrations n_{ai} , the wavelength λ , the incident X-ray flux I_0 , and the integration time Δt . From this follows

$$d \propto \sqrt[4]{\frac{P}{r_e^2 \lambda^2 I_0 \Delta t}}$$

for the maximum achievable resolution with a detector with $N \times N$ pixels whose edge is located at $q_{\text{max}} = N \frac{\Delta q}{2}$.

Preliminary Conclusions

1. **Displacement $|POI - POD|$** scales proportional to the sensor thickness
 $\Delta X = \tan(2\theta) d$ $\Delta X > 50 \mu\text{m}$ for $2\theta > 5.7^\circ$
2. **Reduction of the signal-to-noise ratio** depending on the scattering angle and pixel size
3. **Reduction of the sample resolution** by a factor of up to ≈ 2.7 for a planar detector geometry covering $2\theta_{\text{max}} = 60^\circ$ at 12 keV and $50 \mu\text{m}$ pixels.
4. **Reduction of the image contrast** scaling with 2θ , the pixel size and photon energy
5. **Blurring of the image** scaling with the photon energy, scattering angle 2θ and pixel size

References

1. T. Rüter et al., IEEE NSS MIC (2017), pp. 1–3
2. Crillo, I. (2008). *Small-Angle Neutron Scattering and Applications in Soft Condensed Matter*, pp. 723–782, Springer, Heidelberg
3. Starodub, D. (2007). *J. Synchrotron Rad.*, 15, 62–73
4. Henke, B. L. & DuMond, J. W. M. (1955). *J. Appl. Phys.* 26, 903–917
5. Howells, M. R., Beetz, T., Chapman, H. N., Cui, C., Holton, J. M., Jacobsen, C. J. et al. (2005). *arxiv.org* e-print archive, <http://arxiv.org/pdf/physics/0502059>

